REPORT DOCUMENTATION PAGE

Form Approved
OMB No. 0704-0188

Public reporting burden for this collection of information is estimated to average 1 hour per response, including the time for reviewing instructions, searching data sources, gathering and maintaining the data needed, and completing and reviewing the collection of information. Send comments regarding this burden estimate or any other aspect of this collection of information, including suggestions for reducing this burden to Washington Headquarters Service, Directorate for Information Operations and Reports, 1215 Jefferson Davis Highway, Suite 1204, Arlington, VA 22202-4302, and to the Office of Management and Budget, Paperwork Reduction Project (0704-0188) Washington, DC 20503.
PLEASE DO NOT RETURN YOUR FORM TO THE ABOVE ADDRESS.

1. REPORT DATE *(DD-MM-YYYY)*	2. REPORT TYPE	3. DATES COVERED *(From - To)*
15/09/2010	Final	19 Oct-06 to 31-May-2010

4. TITLE AND SUBTITLE
The nanocrystalline state of Narrow Gap Semiconducting chalcogenides

5a. CONTRACT NUMBER

5b. GRANT NUMBER
N00014-07-1-0179

5c. PROGRAM ELEMENT NUMBER

6. AUTHOR(S)
Mercouri G. Kanatzidis

5d. PROJECT NUMBER
07PR02556-00

5e. TASK NUMBER

5f. WORK UNIT NUMBER

7. PERFORMING ORGANIZATION NAME(S) AND ADDRESS(ES)
Northwestern University

8. PERFORMING ORGANIZATION REPORT NUMBER

9. SPONSORING/MONITORING AGENCY NAME(S) AND ADDRESS(ES)
Office of Naval Research

10. SPONSOR/MONITOR'S ACRONYM(S)
ONR

11. SPONSORING/MONITORING AGENCY REPORT NUMBER

12. DISTRIBUTION AVAILABILITY STATEMENT
Approved for public release; distribution unlimited

13. SUPPLEMENTARY NOTES
The views, opinions and/or findings contained in this report are those of the author(s) and should not be construed as an official Department of the Navy position, policy or decision, unless so designated by other documentation

14. ABSTRACT
The proposed program developed synthetic routes to nanocrystalline narrow band gap semiconductors relevant to efficient thermoelectric power generation and to a broader set of electronic applications. The investigated materials were selected from a well known class of narrow band gap semiconducting chalcogenides. We assessed the potential of the nanocrystal-derived materials for achieving high performance as thermoelectrics and found that the potential is low because of the inability to dope the nanocrystals. One objective was to investigate their nanocrystalline state (<50 nm), their capacity for doping with alio-valent element and impurities so that we may control and exploit their electrical transport properties for naval related power generation and detection applications. We discovered that nanoparticles exhibit a self-cleaning effect and expel any alio-valent impurities that might act as dopants. We also discovered new semiconductor phases of matter that are stable only when they exist in the nanosize regime and unstable when they exist in the bulk.

15. SUBJECT TERMS
nanoparticles, semiconductors

16. SECURITY CLASSIFICATION OF:			17. LIMITATION OF ABSTRACT	18. NUMBER OF PAGES	19a. NAME OF RESPONSIBLE PERSON
a. REPORT	b. ABSTRACT	c. THIS PAGE			19b. TELEPONE NUMBER *(Include area code)*
unclassified	unclassified	unclassified	unclassified	22	847-467-1541

FINAL REPORT

August 23, 2010

ONR (N00014-07-1-0179)

The Nanocrystalline State of Narrow Gap Semiconducting Chalcogenides

ONR Program Officer:
Dr. Mihal Gross

Professor MERCOURI KANATZIDIS, PI

Northwestern University

Project ending date:
6/31/2010

20101013410

Technical Objectives

The proposed program aimed to develop synthetic routes to nanocrystalline narrow band gap semiconductors and investigate if nanocrystals can be doped with donor and acceptor dopand. General synthetic methods for convenient preparation of these materials were investigated and developed. The investigated materials were selected from a well known class of narrow band gap semiconducting chalcogenides. We assessed the potential of the nanocrystal-derived materials for achieving high performance as thermoelectrics and found that the potential is low because of the inability to dope the nanocrystals. One objective was to investigate their nanocrystalline state (<50 nm), their capacity for doping with alio-valent element and impurities so that we may control and exploit their electrical transport properties for naval related power generation and detection applications. We discovered that nanoparticles exhibit a self-cleaning effect and expel any alio-valent impurities that might act as dopants.

We aimed to:

- Develop synthetic routes to nanocrystals (<20 nm) of narrow band gap thermoelectric semiconductors
- Investigate electronic and detection applications.
- Answer the question: can nanocrystals be doped with alio-valent element and impurities?
- Achieve dielectric state of narrow band gap semiconductors in nanocrystalline state
- Exploit dielectric state to observe unusual or unique physical properties

Technical Approach

- Invent solution synthesis of nanocrystals of narrow gap materials, important examples: $AgPb_mSbTe_{2+m}$ ($2<m<20$), $Pb_{1-x}Sn_xTe$.
- Carry out doping explorations with alio-valent elements (e.g. Sb^{3+}, Ag^{+} doping in PbTe).
- Perform chemical and physical characterization to demonstrate that nanocrystals are undoped

Technical Objectives

The proposed program aimed to develop synthetic routes to nanocrystalline narrow band gap semiconductors relevant to efficient thermoelectric power generation and to a broader set of electronic applications. General synthetic methods for convenient preparation of these materials were investigated and developed. The investigated materials were selected from a well known class of narrow band gap semiconducting chalcogenides. We assessed the potential of the nanocrystal-derived materials for achieving high performance as thermoelectrics and found that the potential is low because of the inability to dope the nanocrystals. One objective was to investigate their nanocrystalline state (<50 nm), their capacity for doping with alio-valent element and impurities so that we may control and exploit their electrical transport properties for naval related power generation and detection applications.

We aimed to:

- Develop synthetic routes to nanocrystals (<20 nm) of narrow band gap thermoelectric semiconductors
- Investigate electronic and detection applications.
- Answer the question: can nanocrystals be doped with alio-valent element and impurities?
- Achieve dielectric state of narrow band gap semiconductors in nanocrystalline state
- Exploit dielectric state to observe unusual or unique physical properties

Technical Approach

- Invent solution synthesis of nanocrystals of narrow gap materials, important examples: $AgPb_mSbTe_{2+m}$ ($2<m<20$), $Pb_{1-x}Sn_xTe$.
- Carry out doping explorations with alio-valent elements (e.g. Sb^{3+}, Ag^{+} doping in PbTe).
- Perform chemical and physical characterization to demonstrate that nanocrystals are undoped

- Measure relevant properties: thermal conductivity, energy gap, photoluminescence, phase change, etc

Nanocrystalline $AgPb_mSbTe_{m+2}$ and Pb_mSnTe_{m+1} material were prepared in reverse micellar assemblies at room temperature conditions. X-ray powder diffraction patterns of the $AgPb_mSbTe_{m+2}$ and Pb_mSnTe_{m+1} nanocrystal are comparable to their bulk analogs suggesting the successful incorporation of Ag, Sb or Sn into PbTe matrix. $AgPb_mSbTe_{m+2}$ nanocrystals exhibit well define band energies in the mid – IR region. Semi quantitative EDS analyses suggest that $AgPb_mSbTe_{m+2}$ and Pb_mSnTe_{m+1} nanocrystals are rich in Pb. However, further quantitative analyses should be preformed to confirm the elemental compositions of as prepared nanocrystals.

Successful synthesis of nanocrystals of the quaternary thermoelectric materials: $AgPb_mSbTe_{m+2}$ (m=1-18). Nanocrystals of $AgPb_mSbTe_{m+2}$ are not phase-segregated by they are solid solutions.

In contrast to pure lead chalcogenides, silver and antimony containing materials, $AgPb_mSbTe_{m+2}$ or LAST-*m* materials (LAST for Lead Antimony Silver Telluride) have been shown to have enhanced thermoelectric performance, with higher figure of merit values (ZT) ranging from 1.2-1.7 at 700 K.[1, 2] Although by many measures bulk LAST-*m* materials behave as solid solutions, high resolution transmission electron microscopy (HRTEM) studies indicate phase-segregation, with the presence of coherent, endotaxially embedded nanodots (that are appear to be rich in Ag and Sb) in the PbTe matrix.[1, 2] Dimensional reduction has been shown to enhance the thermoelectric performance of a material by increasing the boundary scattering of phonons leading to very low thermal conductivities.[3, 4] Hence, the disposition of a nanocrystalline particle inside a solid crystalline matrix (nanostructuring) can increase the thermoelectric performance of bulk LAST materials resulting in higher ZT values.

However, to date, the nature of these nanodots and their full impact on thermoelectric performance is not well understood. Therefore, we are interested in

stuying a series of nanocrystalline LAST materials, which have similar dimensions to the nanodots found in the bulk materials and study them on their own without interference from the matrix. Since the bulk LAST-*m* systems do not form solid solutions and naturally phase-separate on the nanoscale, one key question that arises is would the LAST-*m* nanocrystals phase-separate or would they be solid solutions? This is a fundamental question which has not been answered to date. Hence, this study is focused on the synthesis of quaternary LAST-*m* nanocrystals with a wide range of *m* values and the detailed investigation of their structure on the atomic scale, *i.e.* ordering of Ag and Sb in the nanocrystalline PbTe matrix.

The simper binary nanocrystals of PbS, PbSe, PbTe and Ag_2Te have been well investigated and reported in the literature.[5-7] However, the reports on more complex ternary and quaternary nanocrystalline materials are rare due to difficulties with phase separation, limitations of suitable precursors as well as complications with solubility of precursors in a common reaction medium. As prepared nanocrystals have spherical to irregular geometries and are polydisperse with size distributions from 3-15 nm. The disperesibility of LAST nanocrystals in common organic solvent is poor and attributed to the incomplete surface passivation by the surfactants. In the present work, we report the synthesis of a broad series of high quality, fairly monodisperse LAST-*m* nanocrystals over a wide range of *m* values using a one-pot low temperature synthetic approach. We show that the nanocrystals of LAST-*m* are in fact homogeneous solid solutions and not further nano-segregated. We also show that they are metastable at room temperature and phase-separate into PbTe and $AgSbTe_2$ upon annealing at moderately high temperatures (150-200 °C).

Nanocrystals of $AgPb_mSbTe_{m+2}$ (m = 1-18) with varying atomic compositions were prepared by using oleic acid (OA) as the surfactant and octadecene (ODE) as the reaction medium. This surfactant/solvent combination along with the lead acetate or lead oxide as the Pb precursor have been shown to yield stable, monodisperse lead chalcogenide nanocrystals with spherical to cubic geometries.[6, 7] For the synthesis of LAST nanocrystals lead acetate, antimony acetate and a thiol stabilized silver complex were used as the Pb, Sb and Ag precursors and elemental tellurium dissolved in trioctylphosphine (TOP) was used as the tellurium source. LAST nanoparticles were

synthesized by simultaneously reacting a mixture of lead oleate, antimony oleate and thiol stabilized silver complex with Te/TOP at 150 °C.

$AgPb_mSbTe_{m+2}$ nanocrystals with six different atomic compositions (m = 1-18) were prepared by varying the molar ratio of Pb, Ag and Sb precursors. Nanocrystals with higher m values (m = 4, 6, 8 and 18) form stable colloidal suspensions in most of the common non-polar solvents (hexane, chloroform and toluene). However the stability of the nanocrystal suspensions decreases with decreasing m values. $AgPbSbTe_3$ and $AgPb_2SbTe_4$ nanoparticles are less stable in colloidal solutions and tend to precipitate within 1-2 days. We presume that the poor stability of lower m LAST nanocrystals is due to the low affinity of Sb and Ag towards oleic acid ligands. Hence, at low m values the larger number of Ag and Sb atoms present on the surface of the nanocrystals are weekly passivated by the oleic acid ligands. Consequently, nanocrystals tend to aggregate and precipitate out of the solution. In contrast, at higher m values the nanocrystal surface is rich in Pb and they are strongly passivated by oleic acid ligands.

Powder X-ray diffraction (PXRD) patterns of the LAST nanocrystals suggest that as-prepared nanocrystals were crystalline with characteristic cubic NaCl structure and $Fm\bar{3}m$ space group (Fig. 1a). Diffraction spectra are shifted to larger 2□angles suggesting incorporation of Ag and Sb into the PbTe lattice. The lattice parameters lie between $AgSbTe_2$ and PbTe and decrease systematically from higher to lower m values (Vegard's law is generally obeyed) suggesting a solid solution behavior (Fig. 1b). The average crystallite size calculated based on line broadening of the Bragg reflections are in the range of 7.5 – 13.4 nm.[8] Additionally, we did not observe any impurity peaks that correspond to Ag_2Te, Sb_2Te_3, elemental Ag, Sb or Te.

The elemental compositions of the LAST nanocrystals were measured with energy dispersive spectroscopy in a scanning electron microscope (SEM/EDS) and X-ray fluorescence (XRF) spectroscopy. The results are listed in the Table 1. In general, both EDS and XRF analyses suggest that as-prepared nanocrystals are richer in Pb and Te than the nominal amounts used in the synthesis.

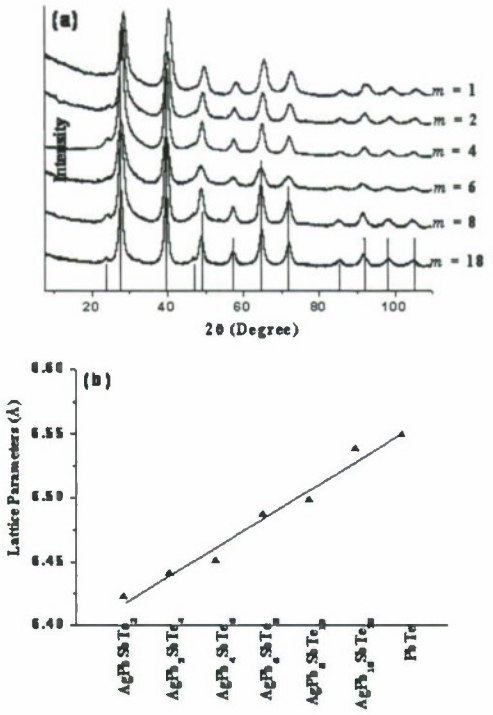

Figure 1. [a] Powder X-ray diffraction patterns of the $AgPb_mSbTe_{m+2}$ (m = 1-18) nanocrystals. The ICDD-PDF overlays of cubic PbTe (PDF # 08-0028) is shown as vertical lines. [b] A plot showing the change in lattice parameter (calculated based on the PXRD spectra) with the nominal atomic composition of $AgPb_mSbTe_{m+2}$ nanocrystals.

Transmission electron microscopy (TEM) images of LAST nanocrystals without any size selective processing are shown in Fig. 2a-e. The as-prepared LAST nanocrystals are nearly spherical in shape and the average particle size is in the range of 8.5 – 14.7 nm for all compositions. Selected area electron diffraction patterns collected from ~ 200 nm^2 area of $AgPb_6SbTe_8$ and $AgPb_4SbTe_6$ nanocrystals (Fig. 2b and 2c insets) show that the main diffraction rings correspond to the NaCl structure type. The lattice fringes in the high resolution TEM image shown in Fig. 2f are those of the (200) plane of $AgPb_6SbTe_8$. In order to confirm that the nanocrystals are a homogeneous single phase, EDS spectral images were collected in scanning transmission electron microscopy (STEM) mode using a 1 nm scanning probe and EDS analysis. STEM image, EDS spectrum and elemental maps recorded from a single $AgPb_4SbTe_6$ nanoparticle are shown in Fig. 3a-f. EDS spectra show the peaks of Ag, Pb, Sb and Te in the single nanoparticle. Elementals maps generated based on the EDS spectra show that Ag and Sb atoms are evenly distributed in the PbTe lattice

confirming the solid solution behavior. Consistent with the elemental maps, the EDS line profiles recorded from a series of $AgPb_4SbTe_6$ nanoparticles in the STEM mode in high resolution SEM (Fig. 3g-h) and the TEM show that Ag, Pb, Sb and Te signals rise and fall together as we move from particle to particle, suggesting that there is no phase separation in the nanoparticles. Similar results were obtained from nanocrystals of $AgPb_6SbTe_8$ and $AgPb_8SbTe_{10}$ which supports the view that nanoparticles obtained from this route are single phase and not a phase separated collection of Ag_2Te, PbTe, Sb_2Te_3 nanocrystals. This observation is in contrast to the bulk quaternary LAST-*m* systems, which are nano-segregated.

The LAST-*m* nanocrystals prepared by this colloidal route exhibit well defined band gap energies in the mid-IR region (Fig. 4). The band gap onset values estimated based on the absorption spectra are in the range of 0.42-0.45 eV. This is consistent with the expected quantum confinement effect where the band gap energies of the nanocrystals are significantly larger than those of the bulk LAST materials (0.26-0.28 eV).[1]

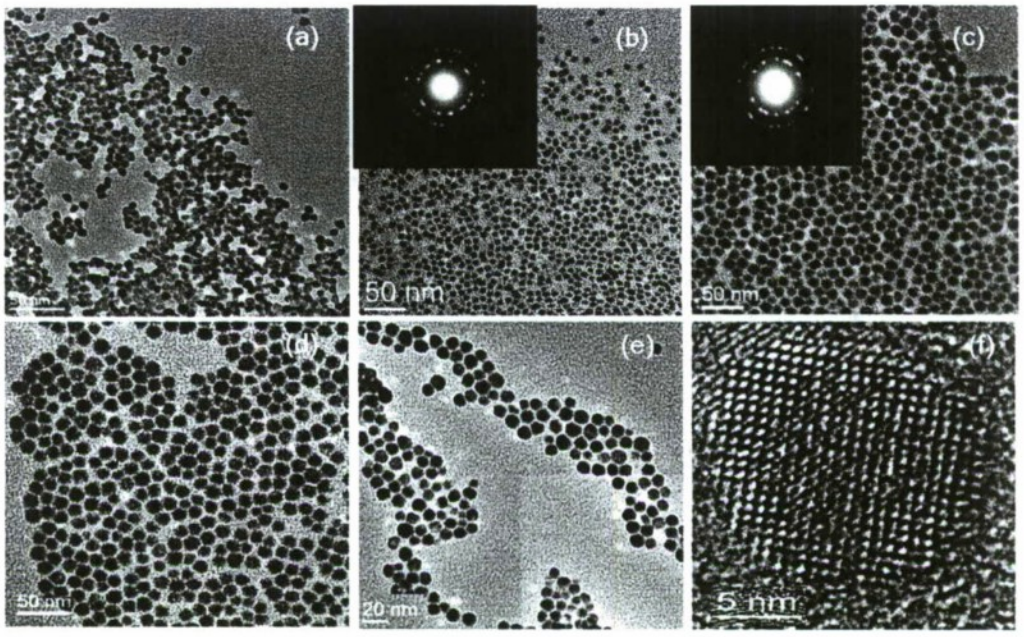

Figure 2. TEM images of the (a) $AgPb_2SbTe_4$ (b) $AgPb_4SbTe_6$ (c) $AgPb_6SbTe_8$ (d) $AgPb_8SbTe_{10}$ (e) $AgPb_{18}SbTe_{20}$ nanocrystals. Insets in (b) and (c) show the selected area electron diffraction pattern from a ~200 nm^2 area of nanocrystals. The diffractions rings are indexable to a cubic $Fm\bar{3}m$ lattice. (f) HRTEM micrograph of $AgPb_6SbTe_8$ nanocrystals from part (c) showing a regular NaCl –type crystal structure viewed down the [200] direction.

The LAST-*m* nanocrystals, which are solid solutions at room temperature tend to phase-separate or segregate at moderately high temperature (150-200°C). PXRD patterns of $AgPb_4SbTe_6$ nanocrystals annealed at 25-100 °C show the growth of crystallite size from 6.3 nm to ~ 14.5 nm without any significant change in the structure. When the $AgPb_4SbTe_6$ nanoparticles are annealed at 150°C for 60 min, however we observed the diffraction peaks of nanocrystalline $AgSbTe_2$ and PbTe suggesting phase separation. Upon further annealing (> 300 °C) for a longer time (> 180 min) the particles tend to phase separate into a mixture of Ag_2Te, Sb_2Te_3 and PbTe. Consistent with the PXRD analyses, differential scanning calorimetric (DSC) analysis of $AgPb_4SbTe_6$ nanoparticles shows two exothermic peaks at ~150 °C and ~300 °C, which corresponds to these phase transitions. These observations are consistent with those of the bulk LAST materials prepared by conventional solid state reactions (>800 °C), which shows the nanoscale segregations of Ag and Sb within the crystalline PbTe matrix.[2]

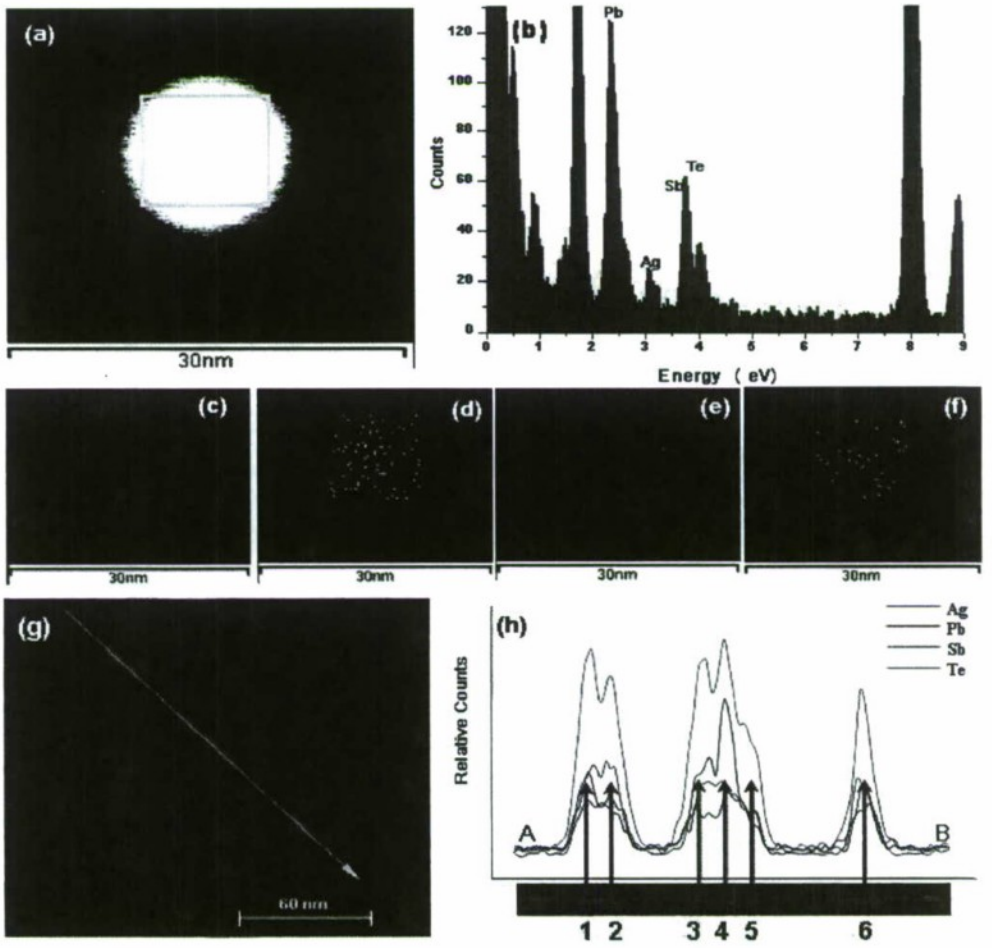

Figure 3. (a) STEM image of $AgPb_4SbTe_6$ nanocrystal acquired in the TEM and the (b) corresponding EDS spectrum showing the presence of all the expected elements in a single nanoparticle. STEM/EDS elemental maps of (c) Ag (d) Sb (e) Pb (f) Te created based on the EDS spectrum. (g) STEM image of $AgPb_4SbTe_6$ nanocrystals acquired in the HRSEM and (h) a line scan through several individual particles (from A to B) showing the presence of all expected elements in $AgPb_4SbTe_6$ nanocrystals.

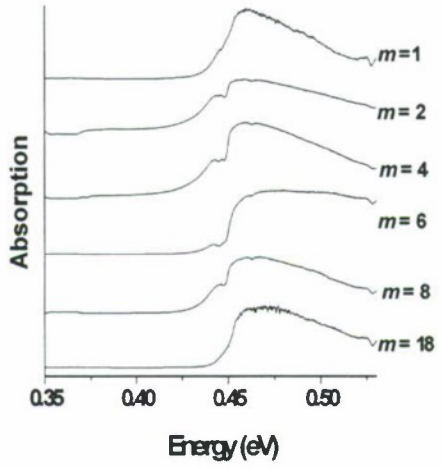

Figure 4. Mid IR absorption spectra of the $AgPb_mSbTe_{m+2}$ (m = 1-18) nanocrystals. All samples were stirred with a 0.5 M hydrazine in acetonitrile solution at 25 °C for 2-3 days and dried under vacuum at 25 °C before the analysis.

In order to find out the morphological and structural changes in nanocrystals upon annealing, we preformed *in-situ* TEM annealing of $AgPb_4SbTe_6$ at 150 °C and 200 °C. $AgPb_4SbTe_6$ nanocrystals deposited on an amorphous carbon coated Cu grid was mounted on a Gatan heating stage and the sample temperature was raised to desired value using a hot stage controller with built-in temperature ramping program. The structural and morphological changes of the nanocrystals were monitored by recording TEM images at regular intervals. The TEM images captured at 150 °C and 200 °C annealed samples (>120 min) show no morphological changes *i.e.* the nanocrystals remain intact, suggesting the phase separation/segregation occurs within the nanocrystals. Consistent with the PXRD analysis, electron diffraction patterns collected from $AgPb_4SbTe_6$ nanoparticles annealed at 150 °C shows the reflections of $AgSbTe_2$ and PbTe.

The entire series of LAST-*m* nanoparticles can be successfully synthesized using a low temperature one-pot colloidal synthetic route. The quaternary nanoparticles are spherical in shape and are fairly monodisperse with absorption band onsets in the mid-

IR region. The LAST-*m* nanoparticles are solid solutions but undergo phase transformation to $AgSbTe_2$ and PbTe at ~150-200°C. Our approach for the synthesis of LAST nanocrystals is cost-effective and facile. It is remarkable that quaternary nanoparticles can be stabilized in this fashion. To our knowledge, the $AgPb_mSbTe_{m+2}$ is the only quaternary system known to successfully produce nanocrystals. It will provide insight for the synthesis of other thermoelectrically relevant ternary and quaternary nanoparticles with control over size and dispersity. The solution stability and processability of these semiconducting nanoparticles makes them useful for thin film preparation and device applications. Hence, we are currently investigating the use of these quaternary nanoparticles for thin film transistors as well as ordered lithographic patterning to make nanoparticle arrays for sensing, photovoltaics and thermoelectric applications.

Table 1. Comparison of nominal and experimental m values, elemental compositions, average crystallite sizes, lattice parameters and optical band gaps of $AgPb_mSbTe_{m+2}$ (m = 1, 2, 4, 6, 8 and 18) nanoparticles.

Nominal m value	Experimental m value [a]	Elemental composition [b]	Crystallite size [nm]	Lattice parameter [Å]	Band gap [eV]
1	2.44	EDS: $Ag_{0.41}PbSb_{0.83}Te_{2.11}$ XRF: $Ag_{0.49}PbSb_{0.97}Te_{2.84}$	6.8 ± 0.2	6.423(2)	0.44
2	3.03	EDS:$Ag_{0.66}Pb_2Sb_{0.89}Te_{3.38}$ XRF: $Ag_{0.61}Pb_2Sb_{0.69}Te_{3.76}$	6.9 ± 0.2	6.441(2)	0.43
4	3.96	EDS: $Ag_{1.01}Pb_4Sb_{1.35}Te_{5.12}$ XRF: $Ag_{0.85}Pb_4Sb_{0.79}Te_{5.67}$	7.6 ± 0.2	6.451(2)	0.43
6	7.69	EDS: $Ag_{0.78}Pb_6Sb_{1.02}Te_{6.10}$ XRF: $Ag_{0.81}Pb_6Sb_{0.92}Te_{6.42}$	8.2 ± 0.2	6.487(2)	0.44
8	9.87	EDS: $Ag_{0.81}Pb_8Sb_{1.08}Te_{9.37}$ XRF: $Ag_{0.72}Pb_8Sb_{0.81}Te_{9.70}$	8.5 ± 0.2	6.498(2)	0.43
18	25.7	EDS: $Ag_{0.7}Pb_{18}Sb_{1.09}Te_{18.87}$ XRF: $Ag_{0.67}Pb_{18}Sb_{0.89}Te_{17.5}$	8.4 ± 0.2	6.539(2)	0.45

[a] Calculated based on the molar ratio of Pb : Ag. [b] Average composition from 5 individual measurements.

References

1. Hsu, K. F.; Loo, S.; Guo, F.; Chen, W.; Dyck, J. S.; Uher, C.; Hogan, T.; Polychroniadis, E. K.; Kanatzidis, M. G., *Science* **2004,** 303, (5659), 818-821.

2. Quarez, E.; Hsu, K. F.; Pcionek, R.; Frangis, N.; Polychroniadis, E. K.; Kanatzidis, M. G., *J. Am. Chem. Soc.* **2005,** 127, 9177-9190.

3. Balandin, A.; Wang, K. L., *J. Appl. Phys.* **1998,** 84, 6149-6153.

4. Khitun, A.; Wang, K. L.; Chen, G., *Nanotechnology* **2000,** 11, 327-331.

5. Hines, M. A.; Scholes, G. D., *Adv. Mater.* **2003,** 21, 1844-1848.

6. Murphy, J. E.; Beard, M. C.; Norman, A. G.; Ahrenkiel, S. P.; Johnson, J. C.; Yu, P.; Micc, O. I.; Ellingson, R. J.; Nozik, A. J., *J. Am. Chem. Soc.* **2006,** 128, 3241-3247.

7. Urban, J. J.; Talapin, D. V.; Shevchenko, E. V.; Kagan, C. R.; Murray, C. B., *Nature Materials* **2007,** 6, (2), 115-121.

8. Borchert, H.; Shevchenko, E. V.; Robert, A.; Mekis, I.; Kornowski, A.; Grubel, G.; Weller, H., *Langmuir* **2005,** 21, 1931-1936.

Forming new compounds as nanocrystals which do not exist in the bulk: The solid solutions $Pb_mSb_nTe_{m+1.5n}$

We achieved the synthesis of a series of monodisperse $Pb_mSb_nTe_{m+1.5n}$ nanocrystals by employing a low temperature colloidal synthetic strategy. Unlike the bulk lead-antimony-telluride materials, as synthesized nanocrystals are solid solutions with cubic NaCl-type structure. These ternary nanocrystals exhibit well defined band energies in the mid-IR region, which are nearly independent from their atomic compositions. $Pb_mSb_nTe_{m+1.5n}$ nanocrystals behave as metastable homogenous solid solutions from 25-200 °C and tend to phase separate into PbTe and Sb_2Te_3 at high temperature conditions (>300 °C).

Bulk lead-antimony-tellurides are a system of two immiscible thermoelectric materials: PbTe-Sb_2Te_3, which exhibit composite structures in the micro and nanometer scale.[9-11] This has been researched by a number of groups as a candidate for thermoelectric devices by utilizing phase transformation reactions such as solidification,[12] eutectoid reactions[13,14] and precipitations.[10] Equilibrium phase diagram of ternary PbTe-Sb_2Te_3 system suggest the formation of an intermediate phase

$Pb_2Sb_6Te_{11}$ which is stable only at a narrow temperature range that is closer to the its' eutectic point.[9,15] However, during a typical solidification process metastable $Pb_2Sb_6Te_{11}$ is formed as the main constituent and the decomposition of that occurs via a eutectoid reaction, requiring long range atomic diffusion. Since the typical solidification processes are too fast for long range atomic diffusion and rearrangements, the resulting intermediate $Pb_2Sb_6Te_{11}$ compound decomposes into binary PbTe and Sb_2Te_3 forming nanoscale lamellar structures of Sb_2Te_3 in the PbTe matrix.[13] Hence, bulk PbTe-Sb_2Te_3 system always behaves as a pseudo-binary system and doesn't form solid solutions at or near room temperature conditions.

Nanocrystalline materials display unique size-tunable physicochemical properties that are distinct from their bulk counterparts.[16,17] Specifically, in nanocrystalline semiconductors, the size-tunable optical and electronic properties are observed because of the quantization of the energy levels.[18-20] Recently, we reported that the more complex ternary and quaternary nanocrystalline materials could display unusual structural and optoelectronic properties that are quite different from their bulk counterparts. Examples include nanocrystalline thermoelectrically relevant materials of $AgPb_mSbTe_{m+2}$, which exhibit solid solution behavior up to 200 °C.[21] Since the PbTe-Sb_2Te_3 system does not form solid solutions at ambient conditions, and naturally phase separate into binary PbTe and Sb_2Te_3, It would be interesting to investigate the nature of the nanocrystalline PbTe-Sb_2Te_3 system with similar atomic composition to their bulk materials, i.e. would they be a solid solution or would they naturally phase separate into binary PbTe and Sb_2Te_3 nanocrystals. Hence, our goal for this work is to synthesize a series of ternary PbTe-Sb_2Te_3 nanocrystals with a range of atomic compositions and the detailed investigation of their structure on the atomic scale. We show that the nanocrystals of PbTe-Sb_2Te_3 are in fact homogeneous solid solutions and not further phase-segregated. We also show that they are metastable at room temperature and phase-separate into binary PbTe and Sb_2Te_3 upon annealing at moderately high temperatures (>300 °C).

Materials: Trioctylphosphine (TOP, 90%), tellurium powder (99.9%), 1-octadecene (90 %), oleic acid (90%), bis[bis(trimethylsilyl)amino]tin(II), lead acetate

trihydrate, antimony acetate, anhydrous ethanol, hexane, carbon tetrachloride, acetone and ethanol were purchased from Aldrich. A 1.0 M Te/TOP solution was prepared in the nitrogen glove box by dissolving 2.552g (20 mmol) of elemental tellurium in 20 mL of TOP at 150 °C. All other chemicals were used without further purification.

Example of Synthesis of $Pb_mSb_nTe_{m+1.5n}$ *nanocrystals:* All syntheses were carried out under air-free conditions using a Schlenk line. In a typical synthesis of ~ 10 nm $Pb_mSb_nTe_{m+1.5n}$ nanocrystals, stoichiometric amounts of lead acetate trihydrate, antimony acetate, 4.0 mL of oleic acid and 20 mL of octadecene was placed in a 100 mL Schlenk flask and dried under vacuum at 100 °C for 3-4 h to obtained a homogeneous colorless solution. The reaction flask was flushed with nitrogen, and the temperature was raised to 180 °C. At 180 °C, appropriate amount of Te/TOP solution (Table 1) was shiftily injected. Upon injection instantaneous nucleation occurs resulting in a brown-black color solution. The temperature of the resulting mixture was maintained at 160-150 °C for 2 min. and the reaction was then cooled to room temperature using an ice-water bath. The resulting nanocrystals were precipitated by adding a mixture of ethanol/hexane (1:1) followed by centrifugation. A black pellet of $Pb_mSb_nTe_{m+1.5n}$ nanocrystals was isolated by pouring off the supernatant solution. The resulting nanocrystals were suspended in chloroform and re-precipitated with ethanol. The purified nanocrystals could be dispersed in hexane, chloroform, carbon tetrachloride or tetrachloromethane to form stable colloidal suspensions. $Pb_mSb_nTe_{m+1.5n}$ nanocrystals with different atomic compositions were prepared by varying the molar ratio of Pb, Sn and Te precursors as shown in the Table 1.

Table 1. The molar ratio of the $Pb(CH_3COO)_2.3H_2O$, antimony acetate and Te/TOP used for the synthesis of $Pb_mSb_nTe_{m+1.5n}$ nanocrystals.

Nominal composition	$Pb(CH_3COO)_2.3H_2O$	$Sb(CH_3COO)_3$	Te/TOP
$PbSbTe_{2.5}$	1.5 mmol, 0.5689 g	1.5 mmol, 0.4476g	3.75 mmol, 0.4785 g
$Pb_2SbTe_{3.5}$	2.0 mmol, 0.7586 g	1.0 mmol, 0.2984 g	3.50 mmol, 0.4466 g
$Pb_4SbTe_{5.5}$	2.4 mmol, 0.9104g	0.6 mmol, 0.1790 g	3.30 mmol, 0.4211g

Characterization: A INEL CPS120 X-ray powder diffractometer with a graphite monochromatized Cu Kα radiation was used for X-ray powder diffraction measurements. Nanocrystal samples were deposited on a glass holder coated with a thin layer of grease and the diffraction patterns were recorded at 20 kV and 40 mA operating conditions. Elemental compositions were obtained using an *in situ* EDS unit (Oxford Inc.) attached to a Hitachi S-3400 scanning electron microscope. Nanocrystal samples were sprinkled on carbon adhesive tabs placed on an aluminum stub, and EDS data were acquired at 25 keV in secondary electron mode. Additionally, an *in situ* EDS unit (Oxford Inc.) attached to the JOEL FasTEM 2100 HR TEM analytical electron microscope is used to further confirm the nanocrystal composition. ICP measurements were carried out by dissolving nanocrystal powder in aqua-regia (HNO_3: HCl, 1:3 volumetric ratio) followed by diluting with ultra pure water. A Thermo Scientific Nicolet 6700 model FT-IR spectrometer is used to record the IR spectra of nanoparticles. All samples were stirred with a 0.5 M hydrazine in anhydrous acetonitrile at 25 °C for 2-3 days to remove the surfactants and vacuum dried at 25 °C for 2 days before the analysis. The transmittance versus wavelength data collected was used to estimate the band gap of the materials by converting transmittance to absorption using Kubelka-Munk fuction.[22] The TEM analyses were conducted in the dark field and bright field modes using a JOEL FasTEM 2100 HR TEM analytical electron microscope operating at an accelerating voltage of 200 kV. Samples were prepared by depositing a drop of nanocrystal suspension in anhydrous hexane or chloroform onto the carbon-coated copper grids and evaporating the solvent. The average particle sizes were manually estimated by measuring the size of 300-400 individual nanoparticles in several TEM images. Elemental maps and the spectral line profiles of the nanocrystals were obtained in STEM mode using a 1 nm scanning probe and the EDS microanalysis. For Annealing studies nanocrystal powder samples were placed in ceramic crucibles and annealed under vacuum at different temperatures for different time periods.

A series of $Pb_mSb_nTe_{m+1.5n}$ nanocrystals was prepared by reacting a mixture of lead oleate and antimony oleate with elemental Te dissolved in TOP. The reaction time was fixed at 2 min. to assure the formation of monodisperse nanocrystals with approximately 10 nm in size. All compositions make highly stable colloidal suspensions

in common non-polar organic solvents. We observed that the amount of Sb incorporated into PbTe lattice can be increased with increasing nominal concentration of antimony. Unlike in the case of $Pb_{1-x}Sn_xTe$, additional surfactants are not necessary to incorporate stoichiometric amount of Sb into the PbTe lattice. We assume that this behavior is because the oleic acid ligands can form strong complexes with both Pb^{2+} and Sb^{3+}, which could ultimately lead to the stabilization of Sb fraction incorporated in to the PbTe matrix.

Powder X-ray diffraction spectra of the $Pb_mSb_nTe_{m+1.5n}$ nanocrystals suggest that as-prepared nanocrystals are highly crystalline with characteristic cubic NaCl-type structure and Fm3m space group (Figure 1A). The diffraction patterns are shifted to larger 2□angles confirming the incorporation of Sb into the PbTe lattice. Lattice parameters calculated based on PXRD measurements show a systematic decrease with increasing Sb concentration (Figure 1B). The average crystallite size calculated based on the line broadening of the Bragg reflections was found to be in the range of 8.6 – 9.1 nm for all compositions.[23] Unlike in the bulk $Pb_mSb_nTe_{m+1.5n}$ we did not observe phase separation or the presences of impurities that correspond to Sb_2Te_3, elemental Pb, Sb or Te.

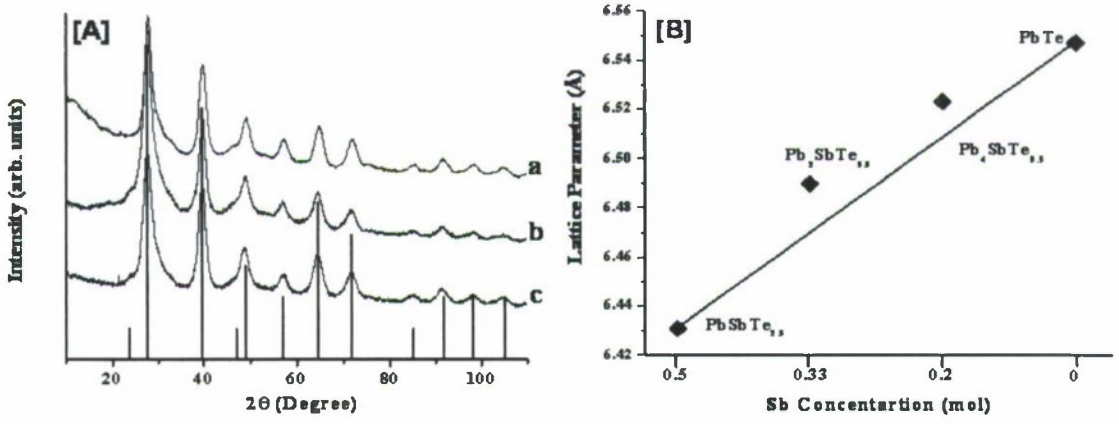

Figure 1. (A) Powder X-ray diffraction spectra of (a) $PbSbTe_{2.5}$ (b) $Pb_2SbTe_{3.5}$, (c) $Pb_4SbTe_{5.5}$ nanocrystals. (B) A Plot showing the change in lattice parameters with Sb concentration. The ICDD-PDF overlays of cubic PbTe (PDF # 08-0028) is shown as vertical lines in part [A].

The elemental compositions of the $Pb_mSb_nTe_{m+1.5n}$ nanocrystals were measured with energy dispersive spectroscopy attached to a scanning electron microscope

(SEM/EDS) as well as using the inductively couple plasma emission spectroscopy (ICP). The average results are listed in the Table 1. In general, both SEM/EDS and ICP analyses suggest that as-prepared nanocrystals are richer in Pb and Te than the nominal amounts used in the synthesis. Nevertheless, the amount of Sb fraction incorporated into PbTe is significant and closer to the nominal composition.

Table 1. Comparison of nominal x values, elemental compositions, average crystallite sizes, lattice parameters and optical band gaps of $Pb_mSb_nTe_{m+1.5n}$ nanoparticles.

Nominal x value	Elemental Composition		Crystallite size [nm]	Lattice parameter [Å]	Band gap [eV]
	EDS[a]	ICP[b]			
$PbSbTe_{2.5}$	$Pb_{1.51}SbTe_{2.9}$	$Pb_{1.67}SbTe_{3.52}$	9.1 ± 0.2	6.431(2)	0.44
$Pb_2SbTe_{3.5}$	$Pb_{2.91}SbTe_{4.31}$	$Pb_{2.6}SbTe_{4.72}$	8.6± 0.2	6.489(2)	0.45
$Pb_4SbTe_{5.5}$	$Pb_{4.13}SbTe_{5.98}$	$Pb_{4.91}SbTe_{5.46}$	8.9± 0.2	6.522(2)	0.43

[a] Average composition from 5 individual measurements from SEM/EDS and TEM/EDS.

[b] Average composition from 3 individual measurements using ICP.

Transmission electron microscopy (TEM) images of $Pb_mSb_nTe_{m+1.5n}$ nanocrystals without any size selective processing are shown in Figure 2a-c. The as-prepared nanocrystals are monodisperse with average particle sizes of 9.5 nm, 9.1 nm and 9.7 nm for $PbSbTe_{2.5}$, $Pb_2SbTe_{3.5}$ and $Pb_4SbTe_{5.5}$ nominal compositions. These values are consistent with the average crystallite size calculations from the PXRD measurements. Selected area electron diffraction pattern collected form a large area of nanocrystals displays the main diffraction spots corresponding to a cubic NaCl-type lattice. Unlike the $Pb_{1-x}Sn_xTe$ nanocrystals prepared in a mixture of octadecene and oleylamine, as synthesized $Pb_mSb_nTe_{m+1.5n}$ nanocrystals are spherical in shape and are highly monodisperse. We assume this behavior is due to the oleic acid ligands which can effectively passivate both Pb^{2+} and Sb^{3+} ions leading to the formation of spherical particles.

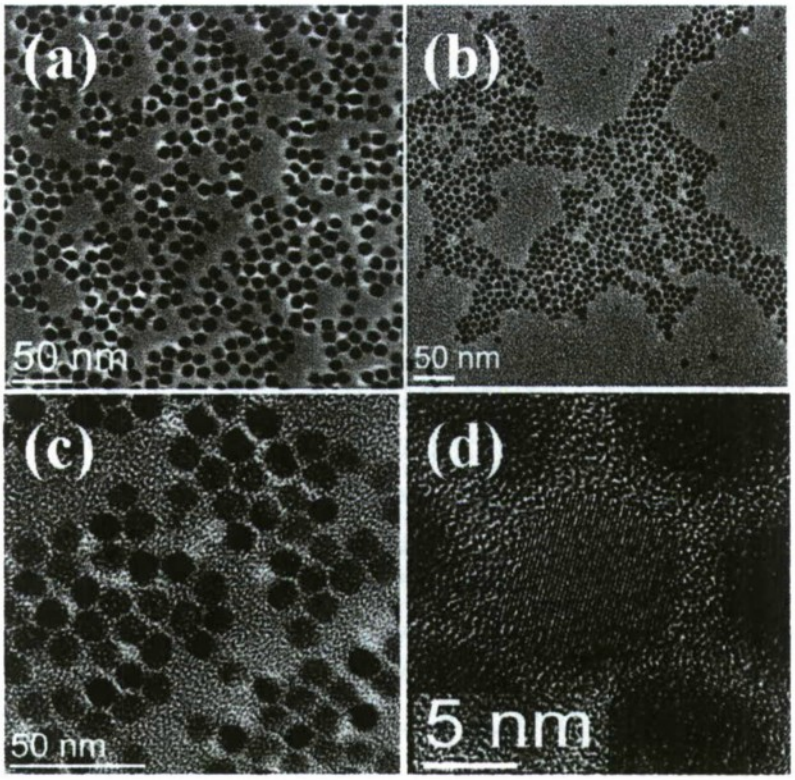

Figure 2. Transmission electron micrographs of the as-synthesized (a) $PbSbTe_{2.5}$ (b) $Pb_2SbTe_{3.5}$, (c) $Pb_4SbTe_{5.5}$ nanocrystals. (d) High resolution TEM image of the $Pb_2SbTe_{3.5}$ nanocrystals from part (b) reflecting the highly crystalline nature of the as synthesized nanocrystals.

In order to confirm that these nanocrystals are homogenous single phase EDS spectral images were collected in scanning transmission electron microcopy using a 1 nm electron probe and the EDS microanalysis. The STEM image, EDS spectrum and the elemental maps generated based on the EDS spectrum of a single $Pb_4SbTe_{5.5}$ nanoparticle are shown in Figure 3a-e. EDS spectra show the peaks of Pb, Sb and Te in the single nanoparticle. Elementals maps generated based on the EDS spectra show that Sb is evenly distributed in the entire PbTe lattice confirming the solid solution behavior. Similar results were obtained from nanocrystals of other compositions which support the view that nanoparticles obtained from this route are homogeneous solid solutions and not a phase separated collection of PbTe and Sb_2Te_3 nanocrystals. This is in sharp contrast to the bulk lead-antimony-telluride materials which are phase segregated.

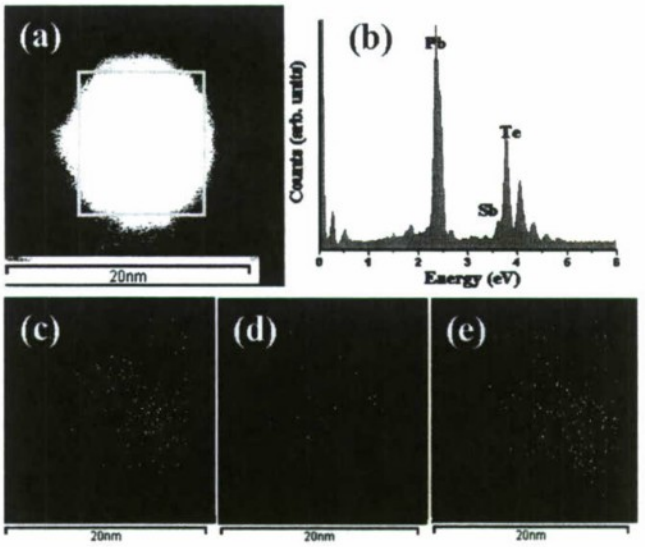

Figure 3. (a) STEM image of $Pb_2SbTe_{3.5}$ nanocrystals and the (b) corresponding EDS spectrum, showing the presence of the expected elements in the nanocrystal. STEM/EDS elemental maps of (c) Pb (d) Sb (e) Te created based on the EDS spectrum.

As synthesized $Pb_mSb_nTe_{m+1.5n}$ nanocrystals exhibit well defined band energy gaps in the mid IR region (Figure 4). The band gap onset values estimated based on the absorption spectra are in the range of 0.42–0.45 eV and found to be nearly independent of the atomic composition. Nevertheless, these absorption onset values are consistent with the expected quantum confinement effect where the band gap energies of the nanocrystals are significantly larger than those of the bulk materials (0.27–0.28 eV).

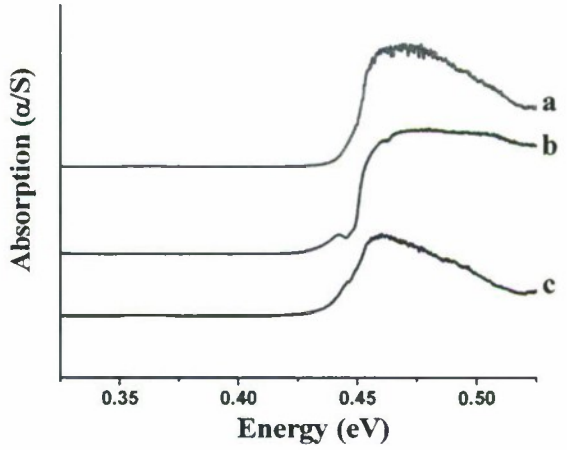

Figure 4. Mid IR absorption spectra of the (a) $PbSnTe_{2.5}$ (red) (b) $Pb_2SbTe_{3.5}$ (blue) and (c) $Pb_4SnTe_{5.5}$ (brown) nanocrystals. All samples were stirred in 0.5 M anhydrous hydrazine for 2-3 days at room temperatures and vacuum dried before the analysis.

The $Pb_mSb_nTe_{m+1.5n}$ nanocrystals, which behave as solid solutions at room temperature, tend to phase-separate or segregate at moderately high temperature (150–200 °C). PXRD patterns of $Pb_4SbTe_{5.5}$ nanocrystals annealed at 25–200 °C for 3-4 h show the growth of crystallite size from 9.1 to -16.5nm without any significant change in the structure. However, when the $Pb_4SbTe_{5.5}$ nanoparticles are annealed at 300 °C for 4 h, we observed the diffraction peaks of nanocrystalline Sb_2Te_3 and PbTe in the PXRD spectrum suggesting phase separation (Figure 5c). These observations are consistent with those of the bulk lead-antimony-telluride materials prepared by conventional solid state reactions, which shows the phase separation.

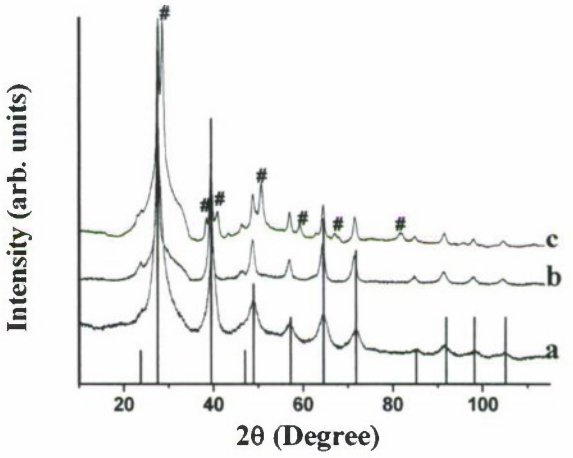

Figure 5. Powder X-ray diffraction spectra of $Pb_4SbTe_{5.5}$ nanocrystals annealed at (a) 25 °C (b) 200 °C and (c) 300 °C for 4 h under vacuum. The ICDD-PDF overlays of cubic PbTe (PDF # 08-0028) is shown as vertical lines. The diffraction peaks marked by # in spectrum (c) corresponds to hexagonal Sb_2Te_3 (ICDD-PDF # 15-0874).

In summary, a series of $Pb_mSb_nTe_{m+1.5n}$ nanoparticles were successfully synthesized by using a low temperature one-pot colloidal synthetic route. The ternary nanoparticles are highly monodisperse with absorption band onsets in the mid-IR region. Structural characterization of nanocrystalline LAST-m suggests that they behave as a metastable solid solution from 25-200 °C and undergo phase transformation to Sb_2Te_3 and PbTe above 300 °C. It is remarkable that ternary lead-antimony-telluride materials can be stabilized in this fashion in the nanometer scale. The contrast between the bulk

materials, which are largely phase-separated, and the corresponding nanodots, which are not, will help guide our future thinking and understanding of the behavior of the bulk systems. It will also provide insight for the synthesis of other thermoelectrically relevant ternary and quaternary nanoparticles with control over size and dispersity. The solution stability and processability of these semiconducting nanoparticles renders them useful for thin film preparation and device applications. Hence, we are currently investigating the use of these quaternary nanoparticles for thin film transistors as well as ordered lithographic patterning to make nanoparticle arrays for sensing, photovoltaics, and thermoelectric applications.

Graduate Students and Postodcs invovled inthis work

Indika Arachchige, Postdoctoral Fellow.

Ronald Roriano, Graduate student.

References:

(1) Nolas, G. S.; Poon, J.; Kanatzidis, M. G. *Mater. Res. Bull.* **2006**, *31*, 199-205.
(2) Dughaish, Z. H. *Physica B.* **2002**, *332*, 205-223.
(3) Konstantatos, G.; Howard, I.; Fischer, A.; Hoogland, S.; Clifford, J.; Klem, E.; Levina, L.; Sargent, E. H. *Nature* **2006**, *442*, 180-183.
(4) Cho, N.; Choudhury, K. R.; Thapa, R. B.; Sahoo, Y.; Ohulchanskyy, T.; Cartwright, A. N.; Lee, K. S.; Prasad, P. N. *Adv. Mater.* **2007**, *19*, 232-236.
(5) Poudel, B.; Hao, Q.; Ma, Y.; Lan, Y.; Minnich, A.; Yu, B.; Yan, X.; Wang, D.; Muto, A.; Vashaee, D.; Chen, X.; Liu, J.; Dresselhaus, M. S.; Chen, G.; Ren, Z. *Science* **2008**, *320*, 634-638.
(6) Hsu, K. F.; Loo, S.; Guo, F.; Chen, W.; Dyck, J. S.; Uher, C.; Hogan, T.; Polychroniadis, E. K.; Kanatzidis, M. G. *Science* **2004**, *297*, 2229-2232.
(7) Quarez, E.; Hsu, K. F.; Pcionek, R.; Frangis, N.; Polychroniadis, E. K.; Kanatzidis, M. G. *J. Am. Chem. Soc.* **2005**, *127*, 9177-9190.
(8) Rowe, D. M. *CRC Handbook of Thermoelectrics*: Boca Raton: CRC, 1995.
(9) Ikeda, T.; Toberer, E. S.; Ravi, V. A.; Snyder, G. J.; Aoyagi, S.; Nishibori, E.; Sakata, M. *Scrip. Mater.* **2009**, *60*, 321-324.
(10) Ikeda, T.; Ravi, V. A.; Snyder, G. J. *Acta Mater.* **2009**, *57*, 666-672.
(11) Ikeda, T.; Ravi, V. A.; Collins, L. A.; Haile, S. M.; Snyder, G. J. *J. Electron. Mater.* **2007**, *36*, 716-720.
(12) Ikeda, T.; Collins, L. A.; Ravi, V. A.; Gascoin, F. S.; Haile, S. M.; Snyder, G. J. *Acta Mater.* **2007**, *55*, 1227.
(13) Ikeda, T.; Collins, L. A.; Ravi, V. A.; Gascoin, F. S.; Haile, S. M.; Snyder, G. J. *Chem. Mater.* **2007**, 763-765.
(14) Ikeda, T.; Ravi, V. A.; Collins, L. A.; Haile, S. M.; Snyder, G. J. *J. Electron. Mater.* **2007**, *37*, 716-720.
(15) Abrikosov, N. K.; Elagina, E. I.; Popova, M. A. *Inorg. Mater.* **1965**, *1*, 1944.
(16) Alivisatos, A. P. *Science* **1996**, *271*, 933-937.

(17) Murray, C. B.; Kagan, C. R.; Bawendi, M. G. *Annu. Rev. Mater. Sci.* **2000**, *30*, 545-610.
(18) Steigerwald, M. I.; Brus, L. E. *Acc. Chem. Res.* **1993**, *23*, 183-188.
(19) Wang, Y.; Herron, N. *J. Phys. Chem.* **1991**, *95*, 525-532.
(20) Trindale, T. O.; O'Brien, P.; Pickett, N. L. *Chem. Mater.* **2001**, *13*, 3843-3858.
(21) Arachchige, I. U.; Wu, J.; Dravid, V. P.; Kanatzidis, M. G. *Adv. Mater.* **2008**, *20*, 3638-3642.
(22) Tandon, S. P.; Gupta, J. P. *Phys. Stat. Sol.* **1970**, *38*, 363-367.
(23) Borchert, H.; Shevchenko, E. V.; Robert, A.; Mekis, I.; Kornowski, A.; Grubel, G.; Weller, H. *Langmuir* **2005**, *21*, 1931-1936.

Relevant Publications generated during this project (2007-2010)

"Nanostructured Thermoelectric Materials" T. Hogan, A. Downey, J. Short, J. D'Angelo, C.-I. Wu, E. Quarez, J. Androulakis, P.F.P. Poudeu, J. Sootsman, D.-Y. Chung, M.G. Kanatzidis, S.D. Mahanti, E. Timm, H. Schock, F. Ren, J. Johnson and E. Case *J. Electron. Mater.* **2007;** 36(7), 704-710.

"Aerogels from metal chalcogenides and their emerging unique properties" S. Bag, I.U. Arachchige, and M.G. Kanatzidis *Journal of Materials Chemistry* **2008** *18* (31), 3628-3632.

"Nanocrystals of the Quaternary Thermoelectric Materials: $AgPb_mSbTe_{m+2}$ (m=1-18): Phase-Segregated or Solid Solutions?" I.U. Arachchige, J.S.Wu, V.P. Dravid, M.G. Kanatzidis, *Advanced Materials* **2008** *20* 3638-+.

"Anomalous Band Gap Evolution from Band Inversion in $Pb_{1-x}Sn_xTe$ Nanocrystals" I.U. Arachchige, M.G. Kanatzidis, *Nano Letters* **2009** *9* (4) 1583-1587.

Entropically stabilized local dipole formation in PbTe Emil S. Boˇzin, Christos D. Malliakas, Petros Souvatzis, Thomas Proffen, Nicola A. Spaldin, Mercouri G. Kanatzidis & Simon J. L. Billinge, Science submitted.

Students supported in part by this grant

Ronald Soriano
In Chung

Postdocs supported in part by this grant

Indika Arachchige
Chris Malliakas

Metadata of the chapter that will be visualized online

Series Title	Structure and Bonding	
Chapter Title	Germanium-Based Porous Semiconductors from Molecular Zintl Anions	
Chapter SubTitle		
Copyright Year	2010	
Copyright Holder	Springer-Verlag Berlin Heidelberg	
Corresponding Author	Family Name	Kanatzidis
	Particle	
	Given Name	**Mercouri G.**
	Suffix	
	Division	Department of Chemistry
	Organization	Northwestern University
	Address	60208, Evanston, IL, USA
	Email	m-kanatzidis@northwestern.edu
Author	Family Name	Armatas
	Particle	
	Given Name	**Gerasimos S.**
	Suffix	
	Division	Department of Materials Science and Technology
	Organization	University of Crete
	Address	71003, Heraklion, Greece
	Email	garmatas@materials.uoc.gr

Abstract	This review highlights how molecular Zintl compounds can be used to create new materials with a variety of novel opto-electronic and gas absorption properties. The generality of the synthetic approach described in this chapter on coupling various group-IV Zintl clusters provides an important tool for the design of new kinds of periodically ordered mesoporous semiconductors with tunable chemical and physical properties. We illustrate the potential of Zintl compounds to produce highly porous non-oxidic semiconductors, and we also cover the recent advances in the development of mesoporous elemental-based, metal-chalcogenide, and binary intermetallic alloy materials. The principles behind this approach and some perspectives for application of the derived materials are discussed.

Keywords (separated by '-')	Chalcogenide - Germanium compound - Mesoporous semiconductor - Self-assembly - Zintl compound